

Article

Adsorption of Polyethyleneimine on Fine Arsenopyrite and the Effect on Its Xanthate Flotation

Pingtian Ming¹, Qingqing Xing^{1,*}, Zhen Wang^{2,*} , Kaile Zhao³, Fei Li¹, Dan Zou² and Youguo Guan¹

¹ Qinghai Engineering Research Center for Gold Mineral Resource Development Dressing and Metallurgy Pilot Plant, Dulan Jin Hui Mining Limited Corporation, Haixi Zhou 816100, China

² Key Laboratory of Solid Waste Treatment and Resource Recycle Ministry of Education, Southwest University of Science and Technology, Mianyang 621010, China

³ Institute of Multipurpose Utilization of Mineral Resources, Chinese Academy of Geological Sciences, Chengdu 610042, China

* Correspondence: xqq20221026@163.com (Q.X.); wangzhen@swust.edu.cn (Z.W.)

Abstract: Effective flotation of fine particles is a problem for mineral processing. In this paper, a flocculant mostly used in heavy metal ion treatment was used in an arsenopyrite flotation system. The adsorption behavior and flotation performance of PEI on the xanthate flotation of arsenopyrite were investigated through zeta potential and adsorbed amount measurements, XPS and size distribution detections, and micro-flotation tests. Zeta potential results showed that the adsorption of 40 mg/L polyethyleneimine (PEI) caused an increase in the zeta potential of arsenopyrite, and had only a slight depression on the further adsorption of SBX, which was further confirmed by the results of the adsorbed amount measurements. However, when the dosage of PEI was 150 mg/L, the adsorption of SBX was strongly depressed. This was because moderate PEI only bridged different arsenopyrite particles, and most of the active sites for the SBX adsorption were still exposed; when PEI was in excess, the mineral particles would be covered so that there were not enough active sites for SBX adsorption. Fe and As on the mineral surface were the adsorption sites for the PEI molecules, which were resolved from the chemical shifts in the As/Fe peaks of the XPS spectra. PEI can increase particle size, and moderate PEI dosage can make the particle size suitable for flotation with SBX where bridging and hydrophobic effects take place. The flotation results showed that $-20\ \mu\text{m}$ arsenopyrite particles had poor flotation recovery with the SBX collector alone, but when they were treated with 40 mg/L PEI, the recovery largely increased. PEI can serve as an effective flocculant for the flocculation flotation of fine arsenopyrite. A comparison model, showing the possible interactions among reagents, particles, and bubbles in the pulp with different PEI dosages, is proposed.

Keywords: flocculant; fine particles; arsenopyrite; adsorption; flotation



Citation: Ming, P.; Xing, Q.; Wang, Z.; Zhao, K.; Li, F.; Zou, D.; Guan, Y. Adsorption of Polyethyleneimine on Fine Arsenopyrite and the Effect on Its Xanthate Flotation. *Minerals* **2022**, *12*, 1390. <https://doi.org/10.3390/min12111390>

Academic Editor: Hyunjung Kim

Received: 4 September 2022

Accepted: 28 October 2022

Published: 31 October 2022

Publisher's Note: MDPI stays neutral with regard to jurisdictional claims in published maps and institutional affiliations.



Copyright: © 2022 by the authors. Licensee MDPI, Basel, Switzerland. This article is an open access article distributed under the terms and conditions of the Creative Commons Attribution (CC BY) license (<https://creativecommons.org/licenses/by/4.0/>).

1. Introduction

Particle size has a great influence on the theoretical research and practical applications of filler and powder materials. Previous studies have shown that particle size has a significant influence on the stiffness, strength, and toughness of layered silicate and carbon nanotube-reinforced polymer nanocomposites [1]. It was found that with the decrease in particle size, the energy gap increased and the electrical conductivity decreased for pure nano TiO₂ prepared by hydrolysis and gelation of titanium isopropoxide [2]. In the mineral processing field, the “Elephant Curve” shows a maximum recovery at around 100 μm and a decrease in the flotation performance for smaller or larger size particles [3].

Particle size is a major parameter in the flotation process, a widely used method in the field of mineral processing [4]. Particles of various sizes behave differently in flotation, directly affecting the recovery, selectivity, and overall performance. Usually, the flotation of fine particles is less effective compared to coarser mineral particles (in a system with a similar bubble size). Fine-grained minerals have higher surface energy,

leading to non-selective reagent consumption, entrainment or entrapment of particles, and instability of bubble–particle aggregates. It is known that the flotation of minerals is particularly successful for a particle size range of approximately 26–125 μm [5,6]. Too fine a particle size will reduce particle–bubble collision efficiency, thus affecting the stability of the foam. Particles that are too large may rupture the bubble film, causing the particles to separate and flow back into the pulp [7]. Therefore, proper particle size should be selected before flotation.

Continuous exploitation causes exhaustion of coarse-grained, easily processed deposits, and now the industry is forced to exploit and process fine-grained, difficult-to-process deposits to meet the global demand. Therefore, the ore must be finely ground to liberate the valuable minerals from gangues. This leads to problems in the flotation process. Increasing the dosage of the collector or removing surface oxidation products is often used to improve the flotation of fine particles, but the reagent consumption tends to be too large [8]. Carrier flotation has a good improvement effect on fine particle flotation performance. However, the dosage of reagents is also high, because, after the recovery of valuable minerals, it also needs to carry out the subsequent separation of valuable particles and carrier particles, resulting in its low universality [9]. Micro-bubble flotation has some disadvantages: it has a low lifting force and a low rising velocity, which result in long flotation times [10]. Selective flocculation can be achieved with flocculants that only adsorb on the targeted mineral particles, for example, on particles that have been made hydrophobic by the adsorption of a collector [11]. This method provides a simpler, cheaper, and probably more widely applicable method for obtaining selectivity. Polyacrylamide is a common flocculant in the sulfide ore flotation (molybdenite) industry, while using polymeric flocculants may affect Mo recovery [12]. In recent years, the introduction of flocculants such as starch-acrylamide and poly (N-isopropyl acrylamide) into the flotation process has been proposed [13]. However, the selectivity of such flocculants is not high. The flotation recovery of gold in fine-disseminated arsenopyrite-type ores also faces the problem of low Au recovery. Further efforts, including the development of new collectors, activators, and flocculants, are being made.

The Wulonggou gold mine is located in Qinghai Province, western China. The ore there is mainly fine disseminated. The element gold mainly exists in metallic sulfides such as arsenopyrite and pyrite, and the distribution ratio of Au in arsenopyrite approximates 70%. Since the disseminated size of arsenopyrite in ore is finer, the grind fineness must be finer so that Au-bearing minerals can be liberated from the gangues; since the flotation recovery of gold is poor, research on new flocculants is underway.

Polyvinyl imine is often used to remove metal cations in wastewater by coordinating with them. The novelty of this paper is utilizing the affinity of polyvinyl imine with metal cations to develop its potential possibility to be used as a flotation reagent [14]. The adsorption, electrokinetic potential, and XPS measurements, as well as size distribution analysis, were conducted to reveal the flocculating mechanism of PEI on fine arsenopyrite.

2. Experimental

2.1. Materials

The massive arsenopyrite was roughly picked from the Wulonggou mine of Dulan Jinhui Mining Co., Ltd. (Haixi Zhou, China). Bulk mineral samples were crushed using a ceramic hammer and carefully hand-picked to obtain the arsenopyrite as pure as possible. Then, it was ground in a ceramic ball mill. Finally, $-20\ \mu\text{m}$ arsenopyrite was obtained by elutriation method [15], and was used for X-ray fluorescent spectroscopy (XRF), X-ray diffraction (XRD), flotation tests, and other detections. The XRF results showed the main elementary composition of arsenopyrite was 43.46% As, 19.64% S, 32.44% Fe, and 98 g/t Au, and the purity was about 95%. The high purity of the arsenopyrite was reconfirmed by XRD pattern (Figure 1) with the corresponding Powder Diffraction File (PDF) data.

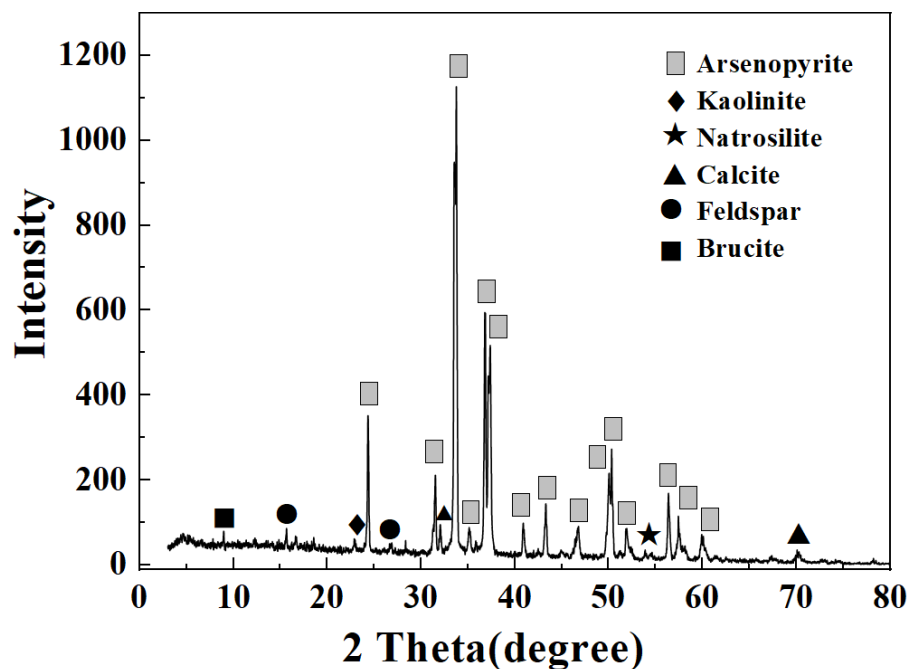


Figure 1. XRD pattern of the sample with the phases being labeled.

The stock solutions of analytically pure sodium hydroxide (NaOH) and sulfuric acid (H_2SO_4) were prepared and used as the pH regulators in all the tests. Sodium butyl xanthate (SBX, 98% purity) was used as the collector in the micro-flotation tests. Polyethyleneimine (PEI, M.W. 10,000, 99% purity) was used as the flocculant. Analytically pure methyl isobutyl carbinol (MIBC) was used as the frother. The monomer (Ethyleneimine) and linear polymer structure are shown in Figure 2. KNO_3 was used as the background electrolyte in zeta potential measurements. Deionized water (with $18.2 \text{ M}\Omega\cdot\text{cm}$ resistivity) was used for all the tests. NaOH, H_2SO_4 , PEI, MIBC, and KNO_3 were obtained from Sinopharm Chemical Reagent (Shanghai, China), and SBX was brought from Tieling flotation reagents Co., Ltd. (Tieling, China).

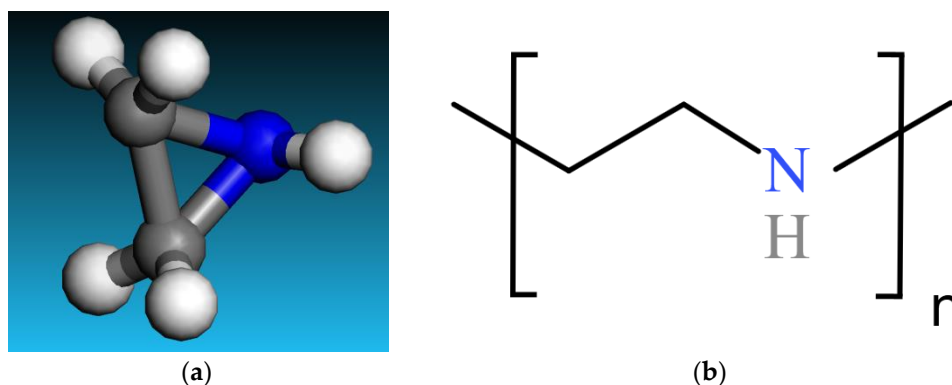


Figure 2. Structure of (a) ethyleneimine monomer and (b) linear polyethyleneimine.

2.2. Electrokinetic Potential Measurements

For electrokinetic measurements, $-20 \mu\text{m}$ of arsenopyrite powder was milled below $5 \mu\text{m}$ in an agate mortar. Then, 20 mg of the $-5 \mu\text{m}$ powder was added into 40 mL of aqueous KNO_3 (1 mM) solution, and conditioned by magnetic stirring for 10 min, with the desired pH regulator and reagent(s) being added separately in sequence. At least 40 min was allowed for the suspension to sediment after stirring stopped. The supernate was used for measuring zeta potentials in a Delsa 440sx Zeta Potential Analyzer. The average of at least three independent experiments was presented.

2.3. Adsorbed Amount Measurements

Briefly, 2.0 g of arsenopyrite powder ($-20\ \mu\text{m}$) and 40 mL of distilled water were added into a 100 mL Erlenmeyer flask. After the addition of the desired amount of PEI into the suspension, the adsorption of PEI and arsenopyrite was allowed to reach equilibrium with 30 min magnetic mixing. Then, SBX was added and the same interaction time was allowed. The suspension was transferred to centrifugal tube to be centrifuged at 4000 r/min. The supernatant was collected for UV spectrometry analysis of the concentration of SBX (301 nm of wavelength [16]), and the adsorbed amount was calculated. All adsorption experiments were performed three times and the average values were reported.

2.4. XPS Detections

Briefly, 1.0 g of $-20\ \mu\text{m}$ arsenopyrite powder was added into the 60 mL micro-flotation cell (just as a mixing container) together with 40 mL distilled water. The pH was adjusted to 7.5, upon which the desired amount of PEI-2 was added, and stirred for 10 min at 1900 r/min. After filtration and vacuum drying, the X-ray photoelectron spectroscopy (XPS) spectra for arsenopyrite samples treated with or without PEI-2 were recorded with a K-Alpha 1063 spectrometer (Thermo Scientific Co., Waltham, MA, USA), which employs Al K α as a sputtering source at 12 kV and 6 mA with 1.0×10^{-9} Pa pressure in the analytical chamber. The curve was fitted using XPSPEAK 4.1 software, developed by a researcher from Taiwan, China [17].

2.5. Particle Size Distribution Analysis

Particle size distribution can directly reflect the flocculation behaviors of arsenopyrite after interacting with PEI-2. The $-20\ \mu\text{m}$ samples were treated with different concentrations of PEI-2 for 3 min to obtain the flocculated suspension. The laser-based particle-size analysis was carried out on the treated and untreated samples with Master-size 2000 instrument (Malvern/England). Ultrasonic was not allowed to be applied to any of the suspensions to prevent damage to the flocs.

2.6. Flocculation Flotation

The micro-flotation tests were conducted in a 60 mL micro-flotation cell. Arsenopyrite particles ($-20\ \mu\text{m}$, 2.0 g) together with 40 mL distilled water were placed into the plexiglass cell to be conditioned for 2 min by stirring at 1900 r/min; then, the pH was adjusted to the needed value, upon which PEI flocculant was added (if needed), followed by SBX collector and MIBC frother (10 mg/L for all the flotation tests); the interval was 3 min between each addition. Then, the flotation was performed for 5 min. The froth and tailings fractions were filtered, dried, and weighed separately. Finally, the arsenopyrite recovery was calculated. Three flotation tests were performed at the same conditions and the average recovery was reported.

3. Results and Discussion

3.1. Surface Charge Property of Arsenopyrite

The influences of flotation reagents on arsenopyrite, e.g., activation, depression, collection, and so on, are generally through the adsorption of corresponding reagent constituents on the mineral surface. This adsorption causes a change in the zeta potential of the arsenopyrite surface [18]. Here, the zeta potential of arsenopyrite was measured before and after treatment with 40 mg/L PEI and 8×10^{-5} M SBX, and the results are shown in Figure 3. Similar to some other reports, pure arsenopyrite PZC was not detected in the pH range 4–11; although, some others presented values of 4, 5.4, etc. [19,20]. This may be related to the different producing areas and the different degrees of oxidation of the arsenopyrite mineral. When arsenopyrite particles interacted with the PEI flocculant, the zeta potential of the arsenopyrite surface increased in the whole pH range, which showed the adsorption of the PEI cations with arsenopyrite. When the pH surpassed 10, the potential variation became small because the concentration of the cationic PEI was low

when strongly alkaline, which was in line with the reported results about dodecyl amine components in solution [21]. After treatment with SBX, the zeta potential of arsenopyrite largely decreased in acidic solution, and more slightly when alkaline, which can be ascribed to the greater adsorption of SBX on the arsenopyrite surface when acidic. It should be noted that the zeta potential variation from Ap to Ap + SBX approximated that from Ap + PEI to Ap + PEI + SBX. This indicated that the pre-adsorbed PEI on the mineral surface only slightly affected the adsorption of SBX in most of the pH range. The adsorbed amount of PEI or SBX could be qualitatively explained by the zeta potential results.

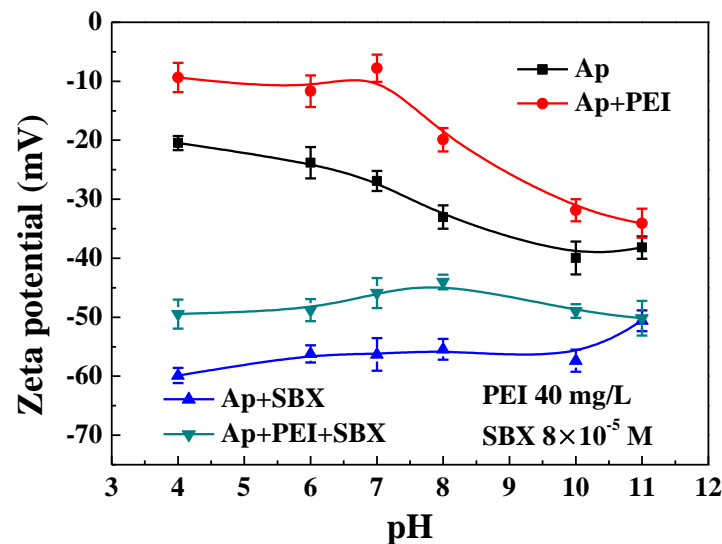


Figure 3. Effects of pH on the zeta potentials of arsenopyrite surface in the presence of 40 mg/L PEI and 8×10^{-5} M SBX (Ap represents arsenopyrite).

3.2. Adsorption Results

In order to quantitatively study the influence of the PEI addition amount on the adsorbed amount of SBX, adsorbed amount measurement tests were conducted. The results are shown in Figure 4. The adsorbed amount of SBX on the arsenopyrite surface increased with the increasing initial concentration (dosage) of SBX. When the initial SBX concentration was greater than 8×10^{-5} M, this trend became unobvious, e.g., the SBX adsorbed amount had a hundred times difference at 4×10^{-5} M and 8×10^{-5} M, but from 8×10^{-5} M to 1.2×10^{-4} M, the adsorbed amount had the same order of magnitude. Generally, by increasing the collector dosage, monolayer adsorption gradually forms, which is responsible for the above trend [22]. When there was 40 mg/L PEI in the solution, the adsorbed amount of SBX only showed a slight decrease at any of the initial SBX concentrations, showing the slight influence of PEI on the adsorption of SBX onto arsenopyrite, which was in line with the results of the zeta potential. If the dosage of the PEI increased to 150 mg/L, the adsorbed amount of SBX on the mineral surface decreased a lot, suggesting that the pre-treatment of excess PEI greatly depressed SBX adsorption. This could be ascribed to the coverage of the polymer PEI on the arsenopyrite surface at high dosages; the steric hindrance brings difficulties to the further adsorption of SBX [23]. This reminds us that a moderate dosage of PEI flocculant may encourage flotation, whereas excess flocculant is just the opposite to one's wishes.

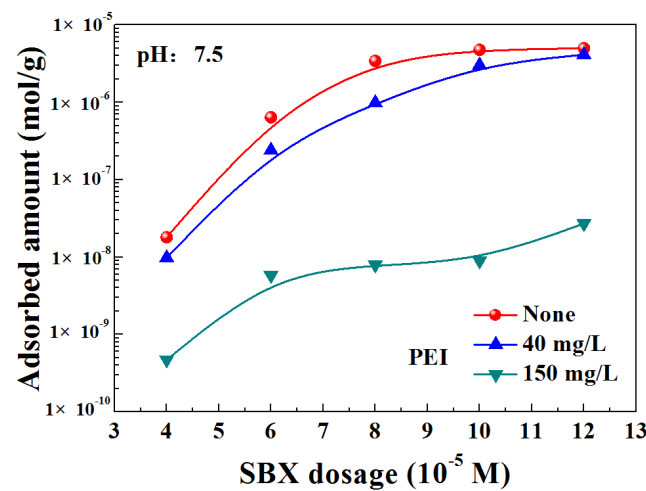


Figure 4. Adsorbed amount of SBX on arsenopyrite surface versus SBX dosage in the presence of 40 mg/L and 150 mg/L PEI (Ap represents arsenopyrite).

3.3. XPS Results

The interaction between the spin magnetic moment and the magnetic field, i.e., spin-orbit coupling, results in the level splitting except for the s level [24]. So, the As 3d and Fe 2p all have two peaks corresponding to 3d 3/2 and 3d 5/2, and 2p1/2 and 2p3/2 energy levels, while the N1s spectra display only one peak. If the interaction between the mineral surface and other matters causes valence electron transfer/sharing, the element chemical shift occurs for the surface element [25]. Here, the XPS spectra of the arsenopyrite surface with and without treatment with PEI were obtained to explain the adsorption mechanism. The elements As, Fe, and N on the arsenopyrite surface-detailed scan spectra are shown in Figure 5. Due to the N element not being present on the arsenopyrite surface, it cannot be detected except for showing some miscellaneous peaks caused by instrumental noise.

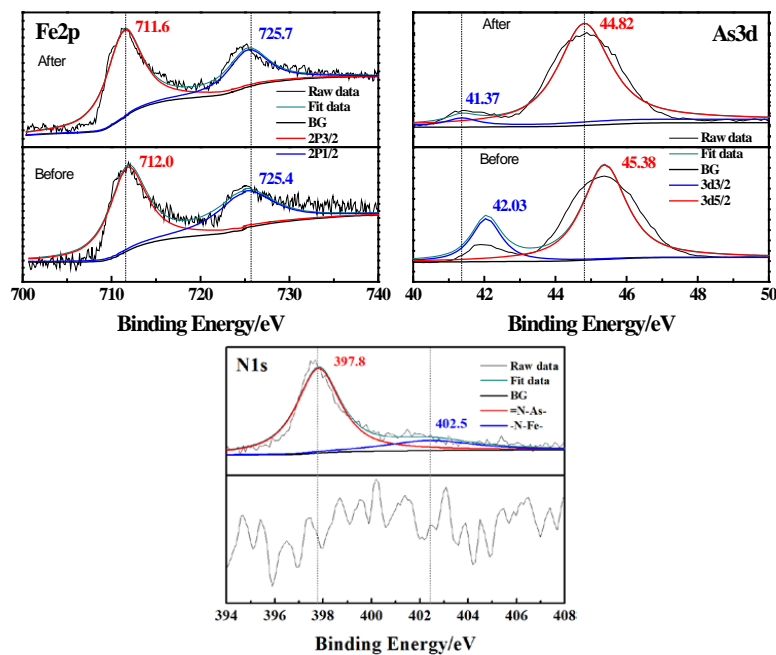


Figure 5. Narrow scanning spectra of Fe, As, and N elements on arsenopyrite surface before and after treatment with PEI.

3.3.1. Chemical Shifts

The splitting levels of elements were obtained from the peak position of the spectra after fitting. The chemical shifts were calculated by the difference in peak position of the same level before and after treatment with PEI, which are shown in Table 1. The N 1s peak occurred at 397.8 and 402.5 eV, and may belong to -N-As- or -N-Fe- bonds [26]. The As 3d 3/2 and 3d 5/2, and Fe 2p1/2 and 2p3/2 levels were located at 41.37, 44.82, 725.7, and 711.6 eV, respectively, which were closer to other research. The chemical shifts in As 3d and Fe 2p were all larger than 0.2 eV. This showed the chemical interaction between the arsenopyrite surface and the PEI molecules. The shifts in As 3d 3/2 and 3d 5/2, and Fe 2p 3/2 were +0.66, +0.56, and +0.4 eV, meaning that the electrons on these levels were attracted by the N of the PEI during the coordination interaction between the N in PEI and the As/Fe atoms on the arsenopyrite surface [27]. Obviously, the adsorption of PEI on the mineral surface was mainly through the coordination between the N atoms and the Fe/As active sites.

Table 1. Binding energies and chemical shifts in Fe, As, and N on arsenopyrite surface.

Peak	Center/eV		Chemical Shift $\Delta E/eV$
	Arsenopyrite	Arsenopyrite + PEI	
N1s	—	397.8	—
As 3d 3/2	41.37	42.03	+0.66
As 3d 5/2	44.82	45.38	+0.56
Fe 2p 3/2	711.6	712	+0.4
Fe 2p 1/2	725.7	725.4	−0.3

3.3.2. Surface Atom Content Variations

The adsorption of reagent on the mineral surface usually leads to variation in the surface atom content, due to the coverage of the molecules. Here, the atom content of Fe, As, S, and N on the arsenopyrite surface with and without PEI treatment was obtained and is provided in Table 2. The Fe, As, and S atom contents on the arsenopyrite surface were detected as 17.78%, 19.38%, and 16.76%, respectively, close to the stoichiometric relationship of [FeAsS]. Before the treatment of PEI, no N element could be detected. When it was treated with PEI, all the contents of the four elements changed, and the variations were −6.04%, −7.43%, −0.80%, and +4.94%, respectively. The surface contents of Fe and As all declined due to the masking effect of the adsorbed macromolecules on Fe/As active sites; although, the S atom content also decreased, the smaller variation value indicated that it was not the main active site for PEI adsorption. The element N from the imino groups in PEI occurred on the treated arsenopyrite surface, which confirmed the adsorption of the flocculant PEI.

Table 2. Content (at. %) of Fe, As, S, and N on arsenopyrite surface.

Samples	Element Content (at.%)			
	Fe	As	S	N
Arsenopyrite	17.78	19.38	16.76	0
Arsenopyrite + PEI	11.74	11.95	15.96	4.94
Variation	−6.04	−7.43	−0.80	4.94

3.4. Detection Results of Particle Size Distribution

PEI was used as a flocculant in this study to regulate the size distribution of the arsenopyrite particles, thus improving flotation recovery. The size distribution curves, including frequency distribution and negative cumulative distribution, of arsenopyrite at different reagent conditions were detected and are shown in Figure 6a–e. After interaction with reagent(s), no significant increase in the content of a single intermediate grain was

observed, meaning that each of the size fractions was subjected to similar flocculation. The corresponding D_{90} , D_{50} , and D_{10} values are shown in Table 3. The values for raw arsenopyrite were 15.09, 11.08, and 7.21 μm , respectively. When it was treated with 40 mg/L PEI solution, all the values increased accordingly, indicating that the flocculation process had taken place. If the concentration of the PEI was 150 mg/L, these values increased substantially to 94.38, 69.26, and 44.99 μm , respectively, which illustrated that larger flocculated particles appeared with the increasing PEI dosage. In flotation, too small or too large particles are not conducive [28]. Which of the two PEI dosages was more suitable remained to be seen by flotation tests. The thing to emphasize is that the relative size of the particles and bubbles has a great influence on flotation, and it does not make much sense to discuss either one in isolation. In our tests, the influence of the PEI on bubble size was very slight.

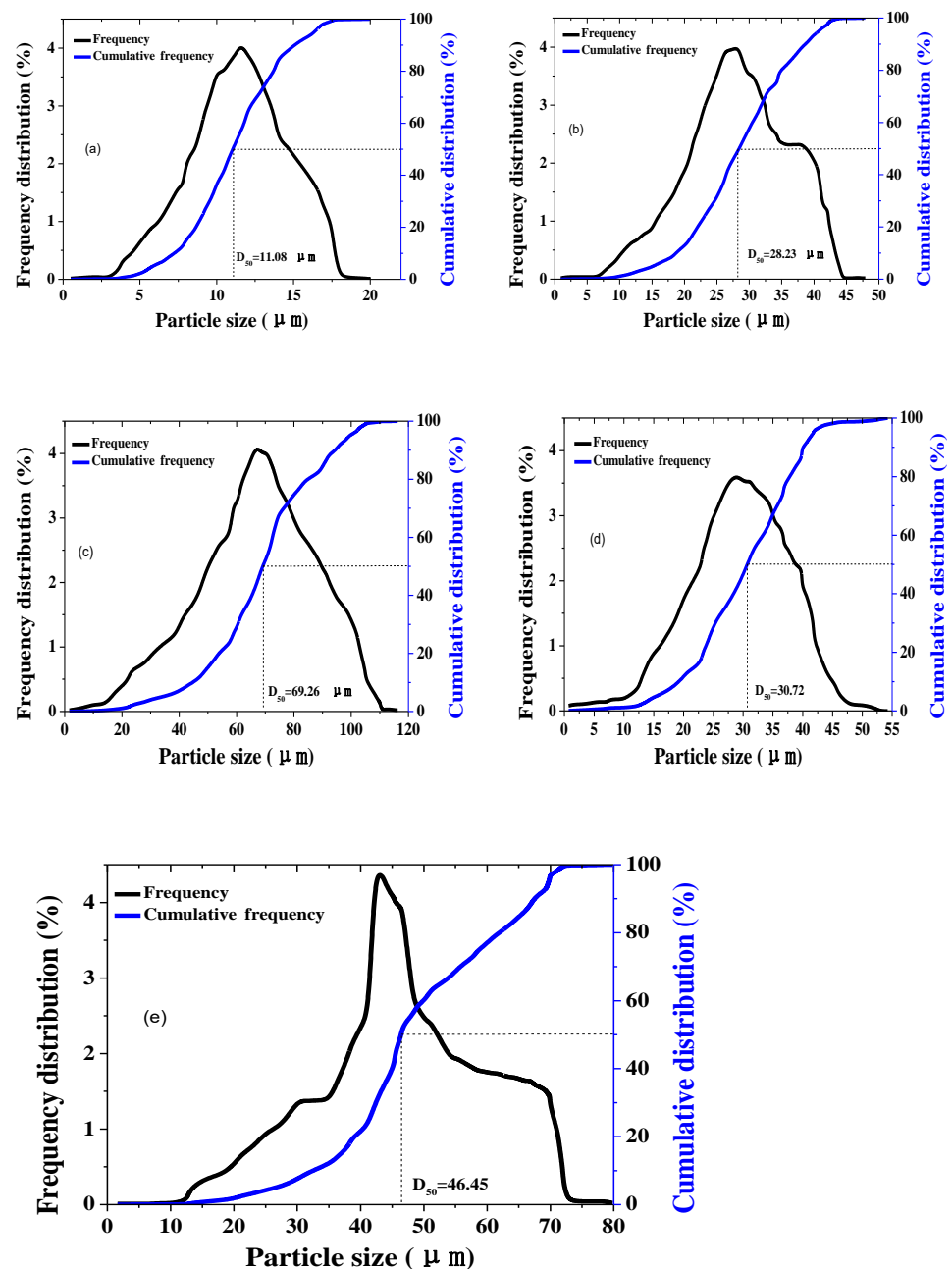


Figure 6. Size distribution curves of arsenopyrite at different reagent conditions. (a) None; (b) 40 mg/L PEI; (c) 150 mg/L PEI; (d) 8×10^{-5} M SBX; (e) 40 mg/L PEI + 8×10^{-5} M SBX.

Table 3. D_{90} , D_{50} , and D_{10} of arsenopyrite particles with and without reagent(s) treatment.

Samples	$D_{90}/\mu\text{m}$	$D_{50}/\mu\text{m}$	$D_{10}/\mu\text{m}$
Arsenopyrite (a)	15.09	11.08	7.21
Arsenopyrite + PEI (b)	38.78	28.23	18.74
Arsenopyrite + PEI (c)	94.38	69.26	44.99
Arsenopyrite + SBX (d)	40.07	30.72	19.20
Arsenopyrite + PEI (40 mg/L) + SBX (e)	67.63	46.45	32.69

When the arsenopyrite particles were treated with only 8×10^{-5} M SBX, the corresponding D_{90} , D_{50} , and D_{10} values also increased, which can be ascribed to the hydrophobic flocculation of SBX. As the mineral surface adsorbs SBX, it becomes hydrophobic, and a hydrophobic attraction occurs between different hydrophobic particles, thus resulting in flocculation [29]. When the arsenopyrite particles were treated with 40 mg/L PEI before 8×10^{-5} M SBX, both the bridging flocculation from the polymer PEI and the hydrophobic flocculation from the SBX prompted the D_{90} , D_{50} , and D_{10} to the values of 67.63, 46.45, and 32.69 μm , accordingly. At this condition, the content of the $-20 \mu\text{m}$ fractions decreased to lower than 2% from 100%; meanwhile, those larger than 74 μm were also lower than 1%, i.e., the ultrafine and oversize particles were all rare, and most of the particles were 20–74 μm ; this may be an ideal granularity range for arsenopyrite flotation.

3.5. Flotation Tests

In order to investigate the influence of particle size variations, resulting from PEI adsorption and flocculation, on fine arsenopyrite ($-20 \mu\text{m}$) flotation performance, pure arsenopyrite flotation tests were carried out. The solution pH, the concentration of PEI, and the dosage of SBX were selected as the variates to study their influence on the flotation. The results are shown in Table 4. With fixed 120 mg/L PEI and 8×10^{-5} M SBX, the maximum 79.84% recovery was accomplished at pH 7.5. This was in line with the reports that PEI exhibited the best flocculation in weak alkaline solution [30]. When the pH and the SBX dosage were fixed at 7.5 and 8×10^{-5} M, it was easy to figure out that with the increasing PEI concentration, the flotation recovery firstly increased then decreased; the flotation reached the optimum 89.67% with 40 mg/L PEI. Comparing this with the results shown in Figure 6, in which 40 mg/L PEI brought flocculated arsenopyrite particles with 28.23 μm D_{50} while 150 mg/L PEI brought it to 69.26 μm , it suggests that oversized flocculated particles were detrimental for flotation. Then, when the SBX dosage effect was separately studied, it was found that recovery increased with the increasing SBX concentration; although, this increase became un conspicuous when the dosage surpassed 8×10^{-5} M.

The key data were drawn in Figure 7 to facilitate observation and analysis. When there was no PEI in the system, the flotation recovery of arsenopyrite was only 44.23%. When 40 mg/L PEI was added before 8×10^{-5} M SBX, the flotation recovery reached 89.67%. The improvement effect of flocculant PEI on the flotation of fine arsenopyrite in the SBX system can be seen clearly. However, when the dosage of PEI was excessive (150 mg/L), it was disadvantageous to the flotation (recovery 32.37%) due to the formation of oversized flocculated arsenopyrite particles (Figure 6). If the SBX dosage was low, the flotation recovery was also not good. Although the recovery of minerals with 1.2×10^{-4} M SBX was best, this only obtained a recovery very slightly higher than those with 8×10^{-5} M SBX. The optimum conditions were still regarded as pH 7.5, PEI 40 mg/L, and SBX 8×10^{-5} M.

Table 4. Conditional tests of fine arsenopyrite flotation.

pH	Systems		Recovery */%
	PEI/mg/L	SBX/ 10^{-5} M	
4	120	8	56.87
6	120	8	64.98
7.5	120	8	79.84
10	120	8	42.3
7.5	0	8	44.23
7.5	10	8	69.87
7.5	40	8	89.67
7.5	80	8	81.13
7.5	150	8	32.37
7.5	40	4	29.36
7.5	40	6	57.76
7.5	40	12	91.22

* The error is within 2%.

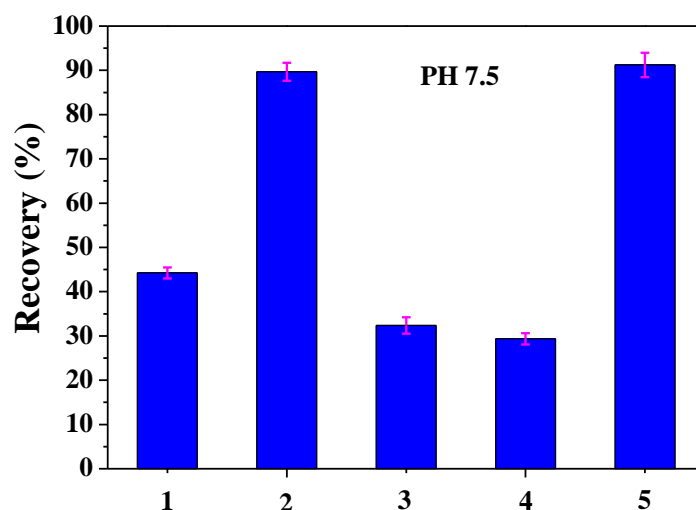


Figure 7. Flotation recovery versus reagent condition at pH 7.5. (1— 8×10^{-5} M SBX; 2—40 mg/L PEI and 8×10^{-5} M SBX; 3—150 mg/L PEI and 8×10^{-5} M SBX; 4—40 mg/L PEI and 4×10^{-5} M SBX; 5—40 mg/L PEI and 1.2×10^{-4} M SBX).

3.6. Mechanism Analysis

We compared the model of the possible states in the pulp that occurred with different PEI dosages in Figure 8. Hydrophobicity and particle size are two important factors affecting the flotation of particles [31]. For condition I, when no PEI was added before SBX, the SBX anions adsorbed on the arsenopyrite surface and resulted in the hydrophobic particles, but due to their small size, the collision probability between the particles and the bubble was low, and thus the recovery was low [32]. For condition II, as moderate PEI (here 40 mg/L) was added into the pulp, its molecules adsorbed several particles and brought forth bridging interactions to flocculate fine arsenopyrite particles to a size suitable for the flotation; meanwhile, there were still enough Fe/As sites for the further adsorption of SBX. For condition III, when excess PEI (here 150 mg/L) was added before SBX, plentiful PEI molecules flocculated the fine particles to oversize ones, which caused the desorption probability from the bubbles to increase [33]; moreover, abundant PEI covered

these particles and occupied the Fe/As sites so that the SBX could not be further adsorbed and the recovery was therefore low.

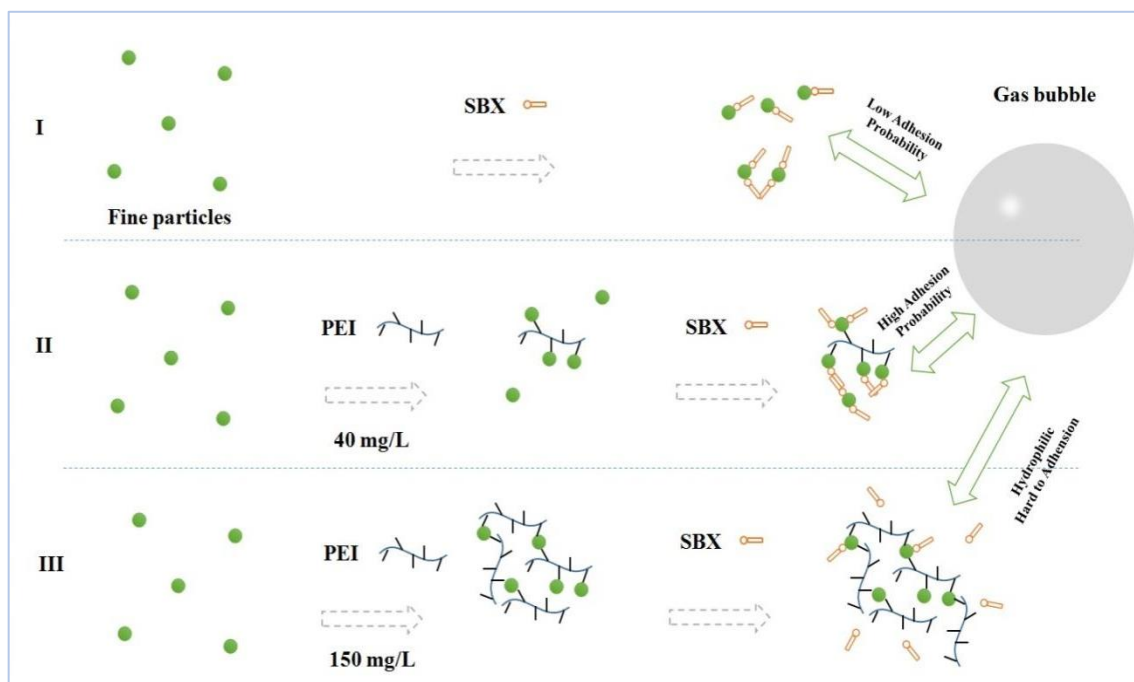


Figure 8. The model of the possible states in the pulp occurred at different PEI dosages.

4. Conclusions

The adsorption of 40 mg/L polyethyleneimine (PEI) caused an increase in the arsenopyrite zeta potential, and it only slightly depressed the further adsorption of SBX. This moderate dosage of PEI only bridged different arsenopyrite particles to larger ones suitable for flotation, leaving most of the active sites on the arsenopyrite surface for SBX adsorption still exposed.

Fe and As on the mineral surface were the adsorption sites for the PEI molecules, inferred from the chemical shifts in the As/Fe peaks of the XPS spectra. PEI can cause the particle size to increase, and a moderate PEI dosage led to the particle size suitable for flotation with SBX. In this process, bridging and hydrophobic effects were all observed, and although $-20\ \mu\text{m}$ arsenopyrite particles had poor flotation recovery in the SBX solution, when they were treated with 40 mg/L PEI, the recovery largely increased. PEI can serve as an effective flocculant for the flocculation flotation of fine arsenopyrite.

Author Contributions: Investigation, P.M., K.Z., F.L. and D.Z.; Data curation, Q.X.; writing—original draft preparation, P.M. and Q.X.; writing—review and editing, Z.W. and Y.G.; project administration, F.L.; funding acquisition, Z.W. and K.Z. All authors have read and agreed to the published version of the manuscript.

Funding: This research was funded by the Sichuan Science and Technology Program of China, grant numbers 2022YFQ0074, 2021YFG0269 and 2022YFS0453. And The APC was funded by [2022YFQ0074].

Data Availability Statement: The data presented in this study are available on request from the corresponding author. The data are not publicly available due to relevant further research is under way.

Conflicts of Interest: The authors declare no conflict of interest.

References

1. Fu, S.Y.; Feng, X.Q.; Lauke, B.; Mai, Y.W. Effects of particle size, particle/matrix interface adhesion and particle loading on mechanical properties of particulate–polymer composites. *Compos. Part. B Eng.* **2008**, *39*, 933–961. [[CrossRef](#)]
2. Avinash, B.S.; Chaturmukha, V.S.; Jayanna, H.S.; Naveen, C.S.; Rajeeva, M.P.; Harish, B.M.; Lamani, A.R. Effect of Particle Size on Band Gap and DC Electrical Conductivity of TiO₂ Nanomaterial. In *AIP Conference Proceedings*; AIP Publishing LLC.: Melville, NY, USA, 2016; Volume 1728, p. 020426.
3. Mankosa, M.J.; Kohmuench, J.N.; Christodoulou, L.; Yan, E.S. Improving fine particle flotation using the StackCell™ (raising the tail of the elephant curve). *Miner. Eng.* **2018**, *121*, 83–89. [[CrossRef](#)]
4. Zhang, X.; Gu, X.; Han, Y.; Parra-Álvarez, N.; Claremboux, V.; Kawatra, S.K. Flotation of iron ores: A review. *Min. Proc. Ext. Met. Rev.* **2021**, *42*, 184–212. [[CrossRef](#)]
5. Kohmuench, J.N.; Mankosa, M.J.; Thanasekaran, H.; Hobert, A. Improving coarse particle flotation using the HydroFloat™ (raising the trunk of the elephant curve). *Miner. Eng.* **2018**, *121*, 137–145. [[CrossRef](#)]
6. Trahar, W.J.; Warren, L.J. The flotability of very fine particles—A review. *Int. J. Miner. Process.* **1976**, *3*, 103–131. [[CrossRef](#)]
7. García-Moreno, F.; Kamm, P.H.; Neu, T.R.; Bülk, F.; Mokso, R.; Schlepütz, C.M.; Stampanoni, M.; Banhart, J. Using X-ray tomography to explore the dynamics of foaming metal. *Nat. Commun.* **2019**, *10*, 3762. [[CrossRef](#)]
8. Wang, W.; Liu, D.; Tu, Y.; Jin, L.; Wang, H. Enrichment of residual carbon in entrained-flow gasification coal fine slag by ultrasonic flotation. *Fuel* **2020**, *278*, 118195. [[CrossRef](#)]
9. Zhang, X.; Hu, Y.; Sun, W.; Xu, L. The effect of polystyrene on the carrier flotation of fine smithsonite. *Minerals* **2017**, *7*, 52. [[CrossRef](#)]
10. Miettinen, T.; Ralston, J.; Fornasiero, D. The limits of fine particle flotation. *Miner. Eng.* **2010**, *23*, 420–437. [[CrossRef](#)]
11. Netten, K.V.; Borrow, D.J.; Galvin, K.P. Fast agglomeration of ultrafine hydrophobic particles using a high-internal-phase emulsion binder comprising permeable hydrophobic films. *Ind. Eng. Chem. Res.* **2017**, *56*, 10658–10666. [[CrossRef](#)]
12. Castro, S.; Laskowski, J.S. Depressing effect of flocculants on molybdenite flotation. *Miner. Eng.* **2015**, *74*, 13–19. [[CrossRef](#)]
13. Zhang, J.; Yang, C.; Niu, F.; Gao, S. Molecular dynamics study on selective flotation of hematite with sodium oleate collector and starch-acrylamide flocculant. *Appl. Surf. Sci.* **2022**, *592*, 153208. [[CrossRef](#)]
14. Ng, W.S.; Sonsie, R.; Forbes, E.; Franks, G.V. Flocculation/flotation of hematite fines with anionic temperature-responsive polymer acting as a selective flocculant and collector. *Miner. Eng.* **2015**, *77*, 64–71. [[CrossRef](#)]
15. Follmer, L.R.; Beavers, A.H. An elutriator method for particle-size analysis with quantitative silt fractionation. *J. Sediment. Res.* **1973**, *43*, 544–549.
16. Zhang, M.; Han, N.; Fei, Y.; Liu, J.; Xing, L.; Núñez-Delgado, A.; Jiang, M.; Liu, S. TiO₂/g-C₃N₄ photocatalyst for the purification of potassium butyl xanthate in mineral processing wastewater. *J. Environ. Manag.* **2021**, *297*, 113311. [[CrossRef](#)]
17. Lu, L.; Xiong, W.; Zhu, Y.; Zhang, X.; Zheng, Y. Depression behaviors of N-thiourea-maleamic acid and its adsorption mechanism on galena in Mo-Pb flotation separation. *Int. J. Min. Sci. Technol.* **2022**, *32*, 181–189. [[CrossRef](#)]
18. Luo, L.; Wu, H.; Xu, L.; Meng, J.; Lu, J.; Zhou, H.; Huo, X.; Huang, L. An in situ ATR-FTIR study of mixed collectors BHA/DDA adsorption in ilmenite-titanaugite flotation system. *Int. J. Min. Sci. Technol.* **2021**, *31*, 689–697. [[CrossRef](#)]
19. Ran, J.; Qiu, X.; Hu, Z.; Liu, Q.; Song, B. Selective Flotation of Pyrite from Arsenopyrite by Low Temperature Oxygen Plasma Pre-Treatment. *Minerals* **2018**, *8*, 568. [[CrossRef](#)]
20. Sirkeci, A.A. Electrokinetic properties of pyrite, arsenopyrite and quartz in the absence and presence of cationic collectors and their flotation behaviour. *Miner. Eng.* **2000**, *13*, 1037–1048. [[CrossRef](#)]
21. Ponou, J.; Wang, L.P.; Dodbiba, G.; Fujita, T. Separation of palladium and silver from semiconductor solid waste by means of liquid-liquid-powder extraction using dodecyl amine acetate as a surfactant collector. *Sep. Purif. Technol.* **2018**, *191*, 86–93. [[CrossRef](#)]
22. Han, C.; Wei, D.; Gao, S.; Zai, Q.; Shen, Y.; Liu, W. Adsorption and desorption of butyl xanthate on chalcopyrite. *J. Mater. Res. Technol.* **2020**, *9*, 12654–12660. [[CrossRef](#)]
23. Wang, Z.; Wu, H.; Yang, J.; Tang, Z.; Luo, L.; Shu, K.; Xu, Y.; Xu, L. Selective flotation separation of bastnaesite from calcite using xanthan gum as a depressant. *Appl. Surf. Sci.* **2020**, *512*, 145714. [[CrossRef](#)]
24. Bernhardt, P.V.; Flanagan, B.M.; Riley, M.J.; Wood, B.J. An XPS study of an isomorphous trivalent lanthanoid series. *J. Electron. Spectrosc.* **2002**, *124*, 73–77. [[CrossRef](#)]
25. Tardio, S.; Cumpson, P.J. Practical estimation of XPS binding energies using widely available quantum chemistry software. *Surf. Interface Anal.* **2018**, *50*, 5–12. [[CrossRef](#)]
26. Majlinger, Z.; Bozanic, A.; Petracic, M.; Kim, K.J.; Kim, B.; Yang, Y.W. NEXAFS and XPS study of GaN formation on ion-bombarded GaAs surfaces. *Vacuum* **2009**, *84*, 41–44. [[CrossRef](#)]
27. Zhou, Z.; Gao, J.; Zhang, G.; Dong, Y.; Wang, Z.; Li, J.; Lyu, J. Optimizing graphene-TiO₂ interface properties via Fermi level modulation for photocatalytic degradation of volatile organic compounds. *Ceram. Int.* **2020**, *46*, 5887–5893. [[CrossRef](#)]
28. Trahar, W.J. A rational interpretation of the role of particle size in flotation. *Int. J. Miner. Process.* **1981**, *8*, 289–327. [[CrossRef](#)]
29. Song, S.; Lopez-Valdivieso, A.; Reyes-Bahena, J.L.; Bermejo-Perez, H.I.; Trass, O. Hydrophobic flocculation of galena fines in aqueous suspensions. *J. Colloid Interface Sci.* **2000**, *227*, 272–281. [[CrossRef](#)]
30. Ba, F.; Foissard, A.; Lebert, A.; Djelveh, G.; Laroche, C. Polyethyleneimine as a tool for compounds fractionation by flocculation in a microalgae biorefinery context. *Bioresour. Technol.* **2020**, *315*, 123857. [[CrossRef](#)]

31. Johansson, G.; Pugh, R.J. The influence of particle size and hydrophobicity on the stability of mineralized froths. *Int. J. Miner. Process.* **1992**, *34*, 1–21. [[CrossRef](#)]
32. Shahbazi, B.; Rezai, B.; Koleini, S.J. Bubble–particle collision and attachment probability on fine particles flotation. *Chem. Eng. Process.* **2010**, *49*, 622–627. [[CrossRef](#)]
33. Zhang, L.; Aziz, N.; Ren, T.; Nemicik, J.; Tu, S. Influence of coal particle size on coal adsorption and desorption characteristics. *Arch. Min. Sci.* **2014**, *59*, 807–820. [[CrossRef](#)]